

UnlinkableDFL: a Practical Mixnet Protocol for Churn-Tolerant Decentralized FL Model Sharing

Chao Feng¹, Thomas Grübl¹, Jan von der Assen¹, Sandrin Raphael Hunkeler¹, Linn Anna Spitz¹,
Gérôme Bovet², Burkhard Stiller¹

¹Communication Systems Group, Department of Informatics, University of Zurich, 8050 Zürich, Switzerland
[cfeng, gruebl, vonderassen, stiller]@ifi.uzh.ch, [sandrinraphael.hunkeler, linnanna.spitz]@uzh.ch

²Cyber-Defence Campus, armasuisse Science & Technology, 3602 Thun, Switzerland gerome.bovet@armasuisse.ch

Abstract—Decentralized Federated Learning (DFL) eliminates the need for a central aggregator, but it can expose communication patterns that reveal participant identities. This work presents *UnlinkableDFL*, a DFL framework that combines a peer-based mixnet with fragment-based model aggregation to ensure unlinkability in fully decentralized settings. Model updates are divided into encrypted fragments, sent over separate multi-hop paths, and aggregated without using any identity information. A theoretical analysis indicates that relay and end-to-end unlinkability improve with larger mixing sets and longer paths, while convergence remains similar to standard FedAvg. A prototype implementation evaluates learning performance, latency, unlinkability, and resource usage. The results show that *UnlinkableDFL* converges reliably and adapts to node churn. Communication latency emerges as the main overhead, while memory and CPU usage stay moderate. These findings illustrate the balance between anonymity and system efficiency, demonstrating that strong unlinkability can be maintained in decentralized learning workflows.

Index Terms—Unlinkability; Anonymous Communication; Decentralized Federated Learning; Mixnets

I. INTRODUCTION

Traditional Machine Learning (ML) keeps all training data in a centralized entity, which leads to growing concerns about data privacy and regulatory compliance [1]. In response, distributed learning methods, such as Federated Learning (FL), have come up as an alternative due to their privacy-preserving and collaborative training mechanisms [2]. In FL, data remain localized in participating nodes. Rather than sharing raw data, nodes exchange local model updates, which are aggregated to facilitate knowledge sharing and improve generalization [3].

In traditional Centralized FL (CFL), local models are sent to a central server for model aggregation. This setup introduces both a single point of failure and aggregation bottlenecks [4]. To address these problems, Decentralized FL (DFL) has been proposed. In DFL, nodes utilize peer-to-peer (P2P) networks to exchange and aggregate their models directly, eliminating the need for a central coordinator. This method removes server-side bottlenecks and lowers the risk of a single point of failure [5]. DFL furthermore provides better flexibility since its network topology can change based on communication patterns or task similarities among nodes [6].

However, the absence of a central coordinator in DFL, while enhancing system availability, also introduces new security and privacy challenges [7]. Without a central entity to manage

authentication, authorization, and accounting, the direct exchange of models between nodes increases the attack surface of the DFL system. Adversaries can link the exchanged model information to the identities of the participating nodes. Recent studies show that even without prior knowledge, analyzing local model updates can reveal the communication topology among nodes [8]. Through this linkability, attackers can identify key nodes and launch malicious attacks, such as distributed denial-of-service (DDoS) or poisoning attacks, to undermine the reliability and dependability of DFL systems.

To counter these threats, improving the reliability and privacy of DFL systems requires enhancing their unlinkability. This means preventing adversaries from linking model updates or communication behaviors to specific node identities while maintaining system availability [9]. However, existing research has mainly focused on privacy and unlinkability in CFL, where a central aggregator manages model updates [10], [11]. These approaches often rely on trusted entities or shuffling mechanisms to blur model origins before aggregation. However, even though these techniques improve network unlinkability, they weaken decentralization of the FL system, which contradicts the fundamental goals of DFL. Therefore, a gap remains in achieving unlinkability in fully decentralized environments.

This paper introduces *UnlinkableDFL*, a DFL framework that integrates anonymous communication into the training workflow. The system contributes:

- A peer-based mixnet architecture integrated into DFL, where each node functions as both learner and relay. Model updates are divided into encrypted fragments. These fragments are sent over randomly routed paths with cover traffic and delays.
- A fragment-based FedAvg method that combines model fragments without revealing identity information. This approach keeps the convergence behavior of standard FedAvg and can handle delayed or missing fragments.
- Support for dynamic topologies, enabling nodes to join or leave during training while maintaining stable routing behavior and consistent aggregated models.
- A theoretical analysis of relay and end-to-end unlinkability, explaining how the outbox size and the path length influence unlinkability under passive observation.
- A prototype implementation and evaluation that examines learning performance, unlinkability, communication

costs, and resource usage. The findings show the trade-off between anonymity and time efficiency.

The remainder of the paper is organized as follows. Section II reviews related work, and Section III introduces the unlinkability problem. Section IV describes the system design, Section V analyzes the system properties, Section VI reports the experimental results, and Section VII concludes the paper.

II. RELATED WORK

This section briefly summarizes relevant prior work on unlinkability in DFL and on mixnets. It reviews existing approaches that address the problem of linking model updates or client identities across training rounds in DFL, as well as network-level anonymity solutions that are based on mixnets.

A. Unlinkability in Federated Learning

The term unlinkability arises from anonymity research and refers to the inability of an adversary to reliably link two or more items, for example, the same user’s actions, across rounds to each other [12]. In an FL setting, unlinkability typically means that a user’s local update in one training round cannot be linked to their participation in another round, or that two gradient-updates cannot be reliably associated with the same client. Although DFL removes the central aggregator, it does not automatically eliminate all linkage risks. Model updates and protocol metadata still carry information that allows adversaries to link updates to a specific identity [13].

The authors of [14] show that in a typical FL setup a malicious central server can reconstruct which users participated in which training rounds (the ‘participant matrix’) by analyzing aggregated model updates over time and auxiliary device-analytics data used for monitoring.

As a potential mitigation, [15] propose an unlinkable FL scheme, which combines a shuffle mechanism that randomly permutes clients’ encrypted updates, with Shamir’s Secret Sharing, which splits each update into multiple shares to prevent the server or adversaries from tracing individual contributions.

AIFL, an anonymity and incentive mechanism, is introduced by [16]. It uses a threshold-based accountable ring signature (TARS) protocol to achieve unlinkability between client identities and their model updates. AIFL further incorporates a detection mechanism based on entropy weighting and cosine similarity to identify malicious or dishonest clients.

The authors of [17] present a framework for dynamic participation in FL that supports anonymous and unlinkable model-update submission. AnoFel integrates cryptographic primitives, anonymity sets, differential privacy, and a public bulletin board to allow users to register and submit model updates anonymously. The framework supports dynamic participation, meaning clients can join or leave at any time without requiring recovery protocols.

B. Mixnets

Mixnets are networks that relay traffic over a sequence of intermediary nodes, often also referred to as mixnodes

or mixes [18], with the goal of enhancing the untraceability and unlinkability of traffic. Each intermediary node applies permutations, delays, paddings or cover traffic to make traffic correlation attacks more difficult [18]. Mixnets were first introduced by [19] in 1981 with the intention of making email traffic less susceptible to traffic analysis. Some drawbacks of the Chaumian mixnet are expensive public-key cryptography and high latency [20]. As a result, hybrid mixnets have been proposed [21], [22], which combine symmetric and asymmetric cryptographic operations to reduce computational overhead.

Since then, different mixnet designs have been proposed, which can be broadly classified into batch and continuous mixnets. One example of a continuous mixnet is Loopix [9], a low-latency anonymous communication system, which uses cover traffic and random delays to achieve strong anonymity guarantees. It delays messages according to a Poisson process, whereas the Chaumian mixnets apply batch mixing and send out messages in discrete rounds. Batch mixing adds significant latency to the system, as compared to Loopix’s continuous mixing, which allows users to tune latency and anonymity. Hence, Loopix is more suitable for real-time communication systems, as compared to Chaumian mixnets. Chaum not only introduced the original mixnet concept but also proposed related systems such as the cMix protocol suite [18]. cMix separates the computationally costly cryptographic operations from the real-time message transmission phase. Servers perform precomputation offline to generate shared secrets and permutations, then use lightweight operations during message transmission.

Applying mixnets to increase the unlinkability in FL systems has been discussed in [10], [23]. Blanco et al. [23] pointed out that applying mixnets to FL has not yet been fully explored in the literature. They discuss Tor, verifiable mixnets and generic peer-to-peer networks as potential options to increase the unlinkability in FL. They also correctly state that applying mixnets to FL systems partly moves the trust problem to a different entity [23].

Jadav et al. [10] introduced FedOnion, which is an Onion Routing-based system for FL, that shares model parameters over an Onion Routing system to increase the anonymity of the model training process. Similarly, [24] and [25] have integrated Onion Routing into an FL system.

However, there is a difference between applying Onion Routing to FL and applying mixnets to FL. Mixnets aim to provide even stronger anonymity guarantees than vanilla Onion Routing. Whereas Onion Routing mainly provides anonymity to source and destination nodes by encapsulating messages in multiple layers of encryption and routing them over a series of relays [10], mixnets also use mixing techniques to resist more advanced forms of traffic analysis by obscuring traffic patterns and using delayed packet forwarding. *Tor*, the most well-known instantiation of Onion Routing, is susceptible to traffic analysis techniques due to non-uniform message sizes and timing [18].

In summary, existing work has explored unlinkability in

FL through cryptographic and protocol-level methods such as update shuffling and secret sharing. However, there is currently little research on applying mixnets to DFL setups. Integrating mixnets into DFL could therefore strengthen privacy guarantees beyond what current cryptographic or aggregation-based approaches achieve.

III. PROBLEM STATEMENT AND THREAT MODEL

This section formalizes the unlinkability problem in DFL systems. It then introduces the corresponding threat model, describing the adversary’s capabilities, goals, and assumptions used throughout the rest of the paper.

A. Problem Statement

Consider a DFL system composed of a set of nodes $\mathcal{N} = \{n_1, n_2, \dots, n_N\}$, interconnected through a P2P network topology $\mathcal{G} = (\mathcal{N}, \mathcal{E})$. Each node n_i owns a private dataset D_i and maintains a local model w_i^t at communication round t . During each round, nodes compute local updates $u_i^t = f(w_i^t, D_i)$ and exchange them with their neighbors, aggregating received updates locally without any global coordination.

A DFL protocol Π specifies how nodes coordinate computation and communication to collaboratively learn a model in a decentralized setting. The goal of the DFL protocol Π is to enable distributed training without sharing raw data or relying on a central aggregator. However, model updates, metadata, and transmission patterns may still leak structural or identity information, necessitating protection against adversarial correlation between exchanged messages and their originating nodes.

During each communication round, nodes generate messages (e.g., model fragments or update packets) and send them through the network. Let Msg denote the set of all transmitted messages. For each $m \in \text{Msg}$, let $S(m) \in \mathcal{N}$ denote its true sender. Let T_b denote the adversary’s observation, consisting of all network-level information available under the threat model in Section III-B.

a) Unlinkability Game: The unlinkability experiment ULink between a challenger and a Probabilistic Polynomial-Time (PPT) adversary \mathcal{A} proceeds as follows:

- 1) *Setup.* The challenger executes Π among nodes in \mathcal{N} with all protocol-defined randomness, traffic shaping, and dummy traffic enabled.
- 2) *Challenge selection.* The adversary chooses two distinct honest nodes $n_a, n_b \in \mathcal{N}$ and selects an admissible target message position j , inducing two possible worlds:

$$\mathcal{W}_0 : S(m_j) = n_a, \quad \mathcal{W}_1 : S(m_j) = n_b. \quad (1)$$

- 3) *Execution.* The challenger samples $b \leftarrow \{0, 1\}$ uniformly and executes \mathcal{W}_b . The adversary receives T_b , the observation generated under \mathcal{W}_b .
- 4) *Decision.* The adversary outputs a bit b' .

b) Adversarial Advantage: The output of the unlinkability game is a bit b' produced by the adversary. The adversary succeeds when $b' = b$, where b determines which world (\mathcal{W}_0 or \mathcal{W}_1) was executed. The advantage quantifies how much better \mathcal{A} performs than random guessing:

$$\text{Adv}_{\Pi}^{\text{ULink}}(\mathcal{A}) = \left| \Pr[b' = b] - \frac{1}{2} \right|. \quad (2)$$

An advantage of 0 means that the adversary can do no better than a random guess, and therefore gains no information about the sender of the challenge message. A non-negligible advantage indicates that the adversary can distinguish the two worlds with meaningful success, implying that message origins are linkable. A protocol achieves sender–message unlinkability when this advantage is negligible for all PPT adversaries.

c) Security Notion: A DFL protocol Π achieves *sender–message unlinkability* if for every PPT adversary \mathcal{A} , $\text{Adv}_{\Pi}^{\text{ULink}}(\mathcal{A})$ is negligible. That is, the origin of m_j cannot be linked to either n_a or n_b with probability noticeably better than random guessing.

B. Threat Model

a) Adversary Type: The adversary \mathcal{A} is *honest-but-curious* and may act as a global network observer or control a limited subset of compromised nodes $\mathcal{C} \subset \mathcal{N}$. \mathcal{A} follows the protocol but seeks to infer sensitive relationships from observed traffic.

b) Adversary Capabilities: The adversary \mathcal{A} is assumed to possess observational capabilities within the network. It can monitor all message transmissions between nodes, including timing information, routing paths, and metadata. In addition, \mathcal{A} may coordinate a subset of compromised nodes to correlate received fragments or updates. The adversary does not possess the cryptographic keys or random parameters that determine the onion encryption and path-selection processes. Additionally, the adversary is passive, meaning it cannot forge, drop, delay, or modify packets, nor can it break cryptographic primitives.

c) Adversary Goals: The main objective of \mathcal{A} is to undermine unlinkability and reveal structural information about the DFL network. Specifically, the adversary attempts to determine whether two or more messages originate from the same node, to associate individual fragments or updates with identifiable participants, and to reconstruct the underlying communication topology \mathcal{G} from observable routing patterns.

d) Defensive Objective: The DFL protocol must maintain unlinkability, ensuring that the adversary’s posterior belief about message origins is indistinguishable from a uniform prior, while maintaining a dependable, adaptive learning process that is efficient in computation and communication.

IV. UNLINKABLEDFL

The *UnlinkableDFL* system operates in a fully decentralized setting where each node performs both FL and mixing functions. Nodes train local models on private data and exchange model fragments with neighbors through a peer-based mixnet. This dual role removes the need for a central coordinator and

allows model aggregation to emerge from local interactions among nodes.

Fig. 1 illustrates the overall workflow of *UnlinkableDFL*. Each node performs both local learning and mixing operations across three layers: the communication layer, the learning layer, and the management layer. Within the communication layer, these fragments are placed into an outbox, mixed with cover messages, and randomly shuffled to increase message entropy. Each fragment is then scheduled for transmission after a random delay, onion-encrypted, and routed through the peer-based mixnet, where intermediate nodes forward and shuffle packets along randomly selected paths. Upon reception, nodes send anonymous acknowledgments using Single-Use Reply Blocks (SURBs), decrypt the received fragments, and buffer them in their local inbox. In the learning layer, each node trains a local model on its private dataset and divides the resulting model into multiple indexed fragments. Neighbor-wise aggregation is then performed using fragment-based FedAvg, combining received fragments with local updates to produce the next model iteration. The management layer oversees deployment and monitoring, maintaining the continuous operation of both the learning and mixing workflows in a decentralized manner.

A. Communication Layer

The communication layer provides the mechanisms through which nodes exchange model fragments over a peer-based mixnet. Its role is to ensure that transmitted updates cannot be reliably associated with their originating nodes. The layer operates independently at each node, handling message preparation, routing, forwarding, and acknowledgment.

Drawing on the design principles of Loopix [9], which uses continuous-time mixing, short independent delays, and cover traffic to limit global traffic analysis, the communication layer of *UnlinkableDFL* adopts a peer-based mixing mechanism for transmitting model fragments. As in the Poisson mixing model of Loopix, fragments are released at random intervals and forwarded over multiple hops, together with cover messages, to reduce sender linkability. Unlike Loopix, which handles stand-alone messages, the communication layer in *UnlinkableDFL* operates within a decentralized learning workflow. It mixes model fragments rather than whole messages, and its routing and timing behavior must support partial delivery and aggregation without affecting the learning process.

a) *Fragment Handling and Outbox Management:*

Model updates are fragmented to avoid exposing the structure or size of the full update through any single message. Each node divides its update into fixed-size fragments and assigns each fragment an index that reflects its position in the model. The index only encodes this position and does not reveal which node generated the fragment or how many fragments were produced for the same update.

All outgoing fragments first enter a local queue, along with relay traffic and SURB-related messages. The queue is a first-in, first-out (FIFO) buffer and does not perform mixing. When the outbox becomes empty, the node moves a fixed number O

of items from the queue into the outbox. If the queue holds fewer than O items, cover messages are added so that the outbox always contains exactly O items. This ensures that each mixing round starts with a minimum batch size.

Once filled, the outbox is randomly permuted using a fresh uniformly sampled permutation over its O entries. The full content of the outbox is reshuffled at every mixing round, so insertion order, burst patterns, and update boundaries are not visible to an observer. After shuffling, items remain in the outbox until released by the transmission scheduler.

b) *Interval Sampling and Transmission Scheduling:*

Randomized intervals are used to decouple outgoing traffic from the timing of local training. If fragments were sent immediately after they are produced, an observer could identify update rounds or detect short-term activity bursts. Interval sampling prevents this kind of timing leakage.

A transmission interval is drawn independently from a truncated normal distribution with configurable mean μ and standard deviation σ . The sampled interval determines when the following item from the (shuffled) outbox becomes eligible for transmission, and a new interval is sampled after each send. This produces a stable outgoing rate while maintaining variability that makes timing patterns less informative.

At each scheduling interval, the node checks whether the currently sampled transmission interval has elapsed. If so, it sends the next item from the shuffled outbox and immediately samples a new interval for the following transmission. Items that are not yet selected simply remain in the outbox and participate in future shuffling rounds, continuing to mix with newly inserted fragments. Cover messages follow the same interval sampling and scheduling logic, preventing idle periods from appearing as observable gaps in the traffic. As a result, the timing of outgoing messages reflects the interval distribution rather than the behavior of the learning process, reducing the adversary's ability to link fragments to update rounds or specific nodes.

c) *Onion Encryption and Multi-hop Routing:*

Before a fragment is transmitted, the node selects a random multi-hop route through the peer network and wraps the fragment in onion encryption. The route length is drawn from a predefined distribution. After determining the number of hops K , the node samples a uniform number of relays from its current routing view, and the resulting sequence forms the path for this fragment. Different fragments choose their routes independently.

For each hop, the node adds one encryption layer that contains only the routing instruction for the next relay. When a relay receives a fragment, it removes a single layer of encryption, reads the next-hop instruction, forwards the remaining payload, and keeps no state linking the incoming packet to any outgoing packet. Relays do not distinguish between real fragments, cover messages, or acknowledgments.

This routing procedure prevents observers from deriving sender-receiver relationships from path structure or forwarding patterns. Independent route selection ensures that fragments from the same update do not follow a predictable path, and onion encryption ensures that relays learn only the mini-

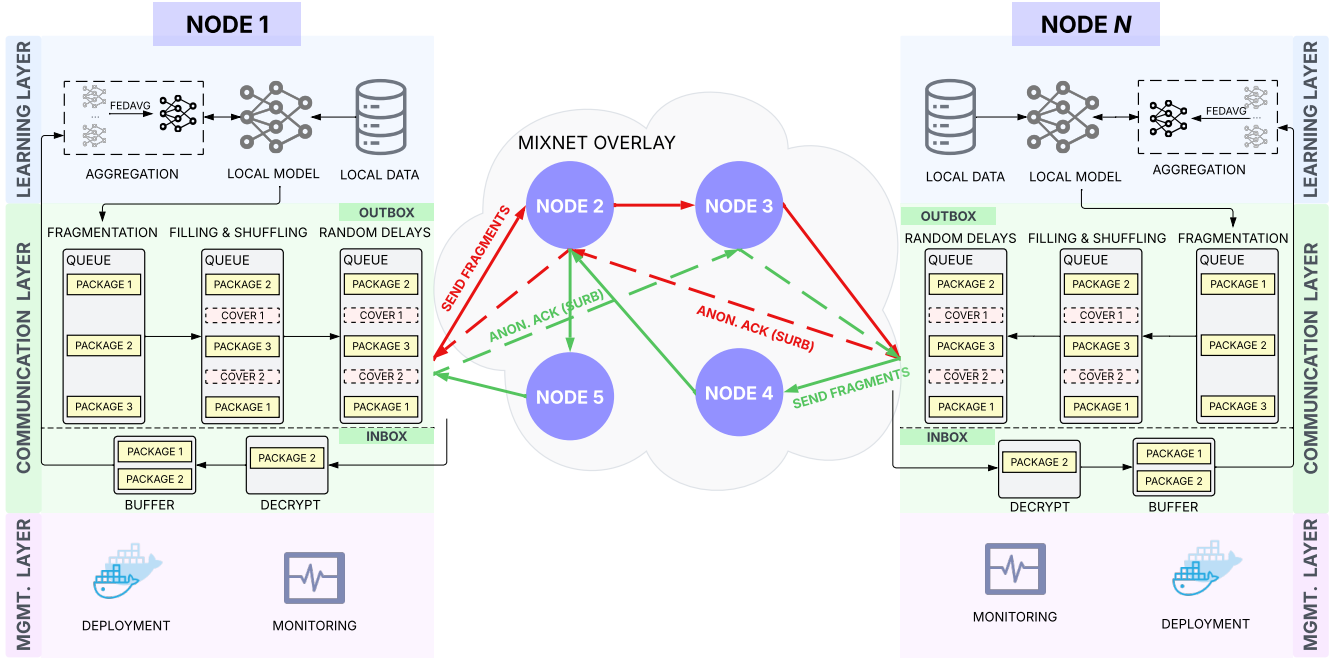


Fig. 1: System architecture of *UnlinkableDFL*. Each node acts simultaneously as a learner and a mixer. Local models are fragmented, shuffled, and transmitted through a peer-based mixnet with stochastic delays and cover traffic. Neighbor-wise aggregation replaces central coordination, while the management layer handles deployment and monitoring.

imum information required to forward the fragment. Together, these properties reduce the amount of routing information available for linkability analysis.

d) Anonymous Acknowledgments: Acknowledgments (ACK) introduce a privacy risk because any direct reply necessarily reveals where the sender of the original fragment can be reached. If an ACK follows the same path as the forwarded fragment, or if it targets the address learned during forwarding, the adversary gains a direct sender–receiver linkage. Even the timing of such replies can expose update boundaries or indicate that multiple packets originate from the same node. A mechanism is therefore needed to allow acknowledgments without disclosing any usable return address.

To address this, the system employs SURBs. When sending a fragment, the originator constructs a SURB that encodes a dedicated return path. This path is chosen independently of the forward path: its hop count is sampled separately, and its relays are selected uniformly from the routing view, so the forward and return routes have no shared structure. The SURB consists of a stack of encryption layers, each containing only the instruction needed for the corresponding hop on the return path. The entire SURB is attached to the fragment as an opaque element that only the sender can later decrypt.

When an acknowledgment is needed, the node generating the ACK does not address the sender directly. Instead, it wraps the ACK in the layers contained in the SURB and forwards the resulting packet along the embedded return path. Each relay performs the same single-layer decryption and

forwarding operation used for normal traffic and learns nothing about either endpoint. Because SURBs are single-use and independent of the forward route, they do not leak any long-term identifiers or structural correlations.

By separating forward and return paths and by encoding the return route entirely within the SURB, acknowledgments avoid becoming an additional linkability channel. They allow fragments to be confirmed without revealing the sender’s location or creating traffic patterns that differ from routine mixnet operation.

e) Cover Traffic Generation: Cover traffic is used to prevent observable gaps in outgoing messages and to hide variations caused by local training activity. Without cover traffic, periods with few or no fragments would produce idle intervals on the wire, allowing an observer to infer when a node is active, when it produces updates, or how many fragments were generated in a round.

Cover messages are generated whenever the outbox requires additional items to reach the configured batch size or when the delay scheduler would otherwise produce an empty transmission interval. These messages follow exactly the same processing steps as real fragments: they enter the queue, participate in outbox shuffling, receive a sampled delay, and are wrapped in onion encryption before being forwarded. Relays do not distinguish between real fragments and cover messages, so both types contribute equally to the observed traffic pattern.

By making cover messages indistinguishable from regular

traffic and by inserting them whenever the outgoing rate would otherwise drop, the system maintains a consistent flow of packets. This prevents external observers from correlating traffic volume or timing with the node’s internal state, reducing the opportunities for linkability based on activity or burst patterns.

B. Learning Layer

The learning layer defines how nodes train local models, exchange information under a dynamic topology, and aggregate updates in the absence of a central coordinator. It operates independently on each node and tolerates asynchronous execution, partial availability, and variable communication delays introduced by the mixing layer. The layer consists of three components: local training, the dynamic topology and asynchronous execution module, and a fragment-based aggregation rule that allows updates to be aggregated even when only a subset of fragments is received.

a) **Local Training:** Each node maintains a local model with the same architecture as all other participants and trains it on its private data using standard optimization methods. Local training proceeds independently on each node, without assuming synchronized rounds or common update intervals. When a node decides to produce an update, it computes a new model state and hands the result to the fragmentation module. The learning layer does not dictate when updates must be computed; nodes may train at different rates depending on their workload, hardware, or availability. This design allows the system to function in heterogeneous environments.

b) **Dynamic Topology and Asynchronous Execution:** Nodes operate in a peer-to-peer environment where participants may join or leave at any time. These events affect both the learning workflow and the routing behavior of the mixing layer. When a node exits unexpectedly, it may still appear in active onion routes. Any packets routed through the exit node will not be decrypted or forwarded, which results in the loss of the corresponding fragments or SURBs. The learning layer treats such losses as normal behavior and does not wait for missing items. To detect node departures, each node maintains periodic connectivity checks to its peers. If a peer fails to respond within a configurable timeout, the peer is marked as inactive. The node is then removed from the local topology view, and no further fragments or SURBs are expected from it. Any items that were routed over the departed peer and remain unacknowledged are resent along newly selected routes.

Joining events are handled through an explicit announcement mechanism. A new node that enters the system broadcasts a join message to its peers, who update their local topology views and propagate the information to others. Once the new node appears in the topology view, it can immediately be used as a relay for packets and can participate in fragment exchange. Because the learning process is asynchronous, on-going updates do not need to be restarted or synchronized. Fragments from the newly joined participant are incorporated as they arrive. Early stopping conditions for aggregation stages are updated dynamically to reflect the current number of

Algorithm 1: Fragment-based FedAvg

Input : Local model W ; set of received fragments \mathcal{C} .

Output: Updated model \tilde{W} .

Step 1: Flatten and initialize.

Flatten W into vector $x \in \mathbb{R}^n$.

Initialize accumulator $a \in \mathbb{R}^n$ and counter $c \in \mathbb{N}^n$.

Set $a \leftarrow x$ and $c \leftarrow \mathbf{1}$. // local model acts as fallback

Step 2: Aggregate received fragments.

foreach *fragment* $f \in \mathcal{C}$ **do**

Let $[s, e)$ be the index range of f .

Let y be the fragment’s values for indices s to $e-1$.

$a[s : e] \leftarrow a[s : e] + y$.

$c[s : e] \leftarrow c[s : e] + 1$.

Step 3: Compute averaged update.

Compute \tilde{x} by elementwise division: $\tilde{x}_i = a_i/c_i$.

Reshape \tilde{x} into model format to obtain \tilde{W} .

return \tilde{W} .

active participants. Through this approach, the learning layer tolerates churn and variations in connectivity without requiring global coordination. Fragments propagate on a best-effort basis, and learning continues even when paths fail, nodes disappear, or new participants join during execution.

c) **Fragment-based FedAvg:** To support partial and asynchronous update exchange, the system performs aggregation at the fragment level. As shown in Algorithm 1, each model is split into fixed-size fragments, and aggregation treats each fragment index as an independent parameter block. Firstly, each node represents its model as a flattened vector and aggregates updates on a fragment-by-fragment basis. Local parameters serve as a fallback: if a fragment for a given index does not arrive, the local value is retained. Incoming fragments are slices of the parameter vector. Whenever a fragment is received, its values are added to the corresponding slice, and a small counter tracks how many contributors were seen for that part of the model. Once all available fragments have been incorporated, each index is averaged over the number of contributors that provided a value for it. The result is then reshaped back into the model. This fragment-based variant of FedAvg allows learning to continue even when only part of an update reaches a node or when the mixing layer delays delivery. It also enables natural integration with dynamic topologies, since different fragments may arrive from different neighbors at various times.

C. Management Layer

The management layer provisions scenarios, maintains node membership, and exposes real-time learning and system metrics. All learning and aggregation decisions remain local to each node. The management layer responsibilities are limited to distributing configuration, tracking node liveness, and pro-

viding observability and control without introducing a central aggregation point.

a) Scenario Deployment: Users utilize the frontend to define scenarios with versioned configurations, including model architecture, fragmentation parameters, routing and delay policies, and resource limits. Nodes retrieve and apply the current configuration independently, allowing updates to be rolled out without pausing ongoing learning.

b) State Monitoring: Each node reports basic status information, including liveness, queue occupancy, outbox activity, send and receive rates, routing statistics, and fragment delivery counters. These metrics provide insight into delay behavior, cover traffic, SURB usage, and fragment retransmissions. The management layer aggregates these reports for inspection, enabling operators to observe load, churn, and routing stability without interacting with the learning layer.

c) Result Presentation: The system presents real-time performance metrics in the frontend, including model accuracy, loss snapshots, fragment coverage, and resource utilization. These metrics help assess whether the learning process progresses despite churn and asynchronous delivery. The management layer offers a unified view of model performance and system behavior across all nodes, supporting debugging, comparison of scenario settings, and post-experiment analysis.

D. Implementation

The system is implemented as a fully containerized DFL platform¹, where each node executes learning, mixing, routing, and monitoring tasks autonomously.

a) Communication Layer: All nodes form persistent bidirectional TCP connections using Docker’s internal DNS. Each node acts as both a server and a client, enabling decentralized communication without a central coordinator. The system handles node churn by monitoring TCP connection health and immediately updating the local view of the topology when connections fail or reappear.

Onion encryption and routing are implemented using the Sphinx cryptographic library, providing encryption, decryption, path construction, and SURBs. Random paths and cover messages rely on Python’s `secrets` module for cryptographically secure randomness. Sphinx uses AES in counter mode to derive per-hop keystreams, while HMAC-SHA256 provides integrity protection for the packet header and payload. The mixer implements temporal unlinkability by shuffling an outbox of size O , sampling transmission intervals from a truncated normal distribution, and generating cover messages when the queue is empty. All outgoing packets are padded to uniform length to prevent size-based correlation.

b) Learning Layer: Local training and fragment-based aggregation are implemented in PyTorch. Models are instantiated as convolutional networks, and datasets are loaded through torchvision. Each node maintains its own training set and applies fragment-based FedAvg during the aggregation stage, using Pytorch’s serialization utilities to flatten and split

parameter tensors into fragments. Incoming fragments are buffered, deduplicated using hash comparisons, and reassembled before global model evaluation.

c) Management Layer: Scenario deployment and node orchestration are implemented using FastAPI for control-plane services and the Python `docker` SDK for container management. The Manager provides REST endpoints for health reporting and maintains a metrics controller that stores and streams metrics via Server-Sent Events (SSE).

V. ANALYSIS OF UNLINKABLEDFL PROPERTIES

This section provides an analysis of the unlinkability and learning properties of *UnlinkableDFL*. Building on the problem and threat model defined in Section III, the analysis quantifies how adversarial observations constrain the identity uncertainty of message senders. It further analyzes how asynchronous execution and fragment-based aggregation affect DFL model convergence.

A. Unlinkability Analysis

This work analyzes how the *UnlinkableDFL* design shapes the adversary’s observation T_b in the unlinkability game of Section III-A, where the adversary must distinguish between $\mathcal{W}_0 : S(m_j) = n_a$ and $\mathcal{W}_1 : S(m_j) = n_b$.

The system first removes appearance-based linkability. All externally visible packets, including model fragments, SURB acknowledgments, and cover traffic, share a uniform size and format. Additionally, onion encryption generates new ciphertexts at each hop, and the outbox applies the same handling to all packet types. Thus, any feature in T_b derived from packet appearance has the same distribution under both worlds. Temporal signals are also homogenized. Each node emits packets according to a truncated-normal renewal law with parameters (μ, σ) , and cover traffic fills idle periods. Before transmission, packets are reshuffled in the outbox. As a result, inter-arrival patterns observed in T_b follow the same distribution independently of the true sender, removing timing-based distinguishing information.

Routing behavior provides no stable sender-dependent signal. Forward paths are selected via onion routing with lengths sampled from $\{1, \dots, K\}$, while SURB-based acknowledgments traverse independently sampled reverse paths. Retransmissions utilize new paths and new SURBs. Thus, relay touchsets, hop counts, and acknowledgment routes appear in T_b according to sender-independent distributions. Payload content and aggregation introduce no identity cues. Fragments contain only model parameters and fixed index positions, and aggregation uses anonymous fragment-level averaging with content-based deduplication. No sender-specific metadata enters T_b through the learning layer.

a) Relay Unlinkability: Relay unlinkability follows from per-hop mixing and local matching probability. Each relay maintains an outbox of size O and applies a uniform shuffle before emission. Under this mechanism, correlating an incoming packet m_i with a specific outgoing packet m_o succeeds with probability at most $\Pr[m_o = m_i] < \frac{K-1}{K} \cdot \frac{1}{O}$, where $1/K$

¹Code available at: <https://anonymous.4open.science/r/PeerBasedMixing>

accounts for paths that terminate at the relay and $\frac{K-1}{K} \cdot \frac{1}{O}$ reflects uniform mixing across O candidates.

Since all packets share identical size and format and follow the same renewal emission schedule, the adversary cannot strengthen this local signal using timing, metadata, or appearance fields.

b) End-to-end Unlinkability: End-to-end unlinkability follows from path diversity and the independence of forward and reverse routes. Forward paths are selected via onion routing with lengths sampled from $\{1, \dots, K\}$, while SURB-based acknowledgments traverse independently sampled reverse paths, while retransmissions utilize new paths and new SURBs. When observing the full network and potentially one compromised relay, the number of feasible end-to-end trajectories are approximately $\sum_{k=1}^K O^k$, yielding path entropy $H_{\text{path}} = \log\left(\sum_{k=1}^K O^k\right)$.

As O grows, the per-hop matching probability decays as $1/O$, while path entropy increases logarithmically in $\sum O^k$. Tracking a packet across multiple hops requires a sequence of per-hop matches. Thus, routing-level signals in T_b are dominated by path randomness rather than sender identity.

Packet-format normalization, timing homogenization, relay mixing, independent path selection, and anonymous aggregation in *UnlinkableDFL* jointly ensure that appearance features, timing characteristics, path-level observations, and payload structure in T_b follow sender-independent distributions. The remaining differences are bounded by the relay-level matching limit and diluted by end-to-end path entropy, yielding adversarial advantage $|\Pr[b' = b] - \frac{1}{2}| = \text{negl}(O, K)$ in the unlinkability game.

B. Convergence Analysis

This subsection examines whether fragment-based aggregation alters the convergence behavior characteristic of FedAvg. The convergence analysis follows the same assumptions used in the analysis of FedAvg and FedAvg-like optimization methods [2], [26], [27]. These assumptions include L -smooth local objectives, unbiased stochastic gradients with bounded variance, and standard control of local model drift.

Let the global objective be

$$F(w) = \frac{1}{N} \sum_{k=1}^N F_k(w), \quad (3)$$

with each F_k being L -smooth. In round t , client k performs τ steps of local SGD with step size η , producing a local model $w_t^{(k)}$. Standard FedAvg updates the i -th coordinate by averaging over the participating set \mathcal{C}_t :

$$\bar{w}_{t,i} = \frac{1}{|\mathcal{C}_t|} \sum_{k \in \mathcal{C}_t} w_{t,i}^{(k)}. \quad (4)$$

In the fragment-based variant, the server receives a collection of index-aligned fragments C_t , where each fragment contains a contiguous segment of some client's model update.

For a given coordinate i , let $c_{t,i}$ denote the number of fragments that contain i , and let $\tilde{w}_{t,i}$ be the aggregated value:

$$\tilde{w}_{t,i} = \frac{1}{c_{t,i}} \sum_{f \in C_t: i \in f} f[i]. \quad (5)$$

If no fragment includes coordinate i ($c_{t,i} = 0$), the algorithm uses a fallback to the pre-aggregation value. Whenever all fragments are available, the update matches FedAvg exactly. With partial availability, the update corresponds to a coordinate-wise average over the clients that contributed fragments covering that coordinate.

To capture this behavior, let $p_{t,i} = \Pr(c_{t,i} \geq 1)$ denote the coverage probability for coordinate i in round t , and define $\bar{p} = \min_i \inf_t p_{t,i}$ as a uniform lower bound on coverage. Similarly, let \bar{K}_{eff} be the minimum expected number of contributors among coordinates that receive at least one fragment. The fallback introduces a bounded deviation represented by Δ_{fb} , which is small when local drift between clients is controlled or when coverage is high.

Under the usual FedAvg step-size condition $\eta \leq 1/(2L)$ and the same local-drift assumptions used in prior work [2], [26], [27], the fragment-based iterate satisfies

$$\frac{1}{T} \sum_{t=0}^{T-1} \mathbb{E} \|\nabla F(\tilde{w}_t)\|^2 = O\left(\frac{1}{\eta T} + \eta L \sigma^2 + \frac{1}{\bar{p} \bar{K}_{\text{eff}} \tau} + (1 - \bar{p}) \Delta_{\text{fb}}\right). \quad (6)$$

The first two terms in Eq. 6 match the rate known for FedAvg. The third term reflects the reduced effective participation caused by fragment-level coverage, and the final term captures the fallback bias when a coordinate receives no fragments. When $\bar{p} = 1$, the fragment-based update is identical to FedAvg and inherits its known convergence rate. As coverage increases, either through more fragments per round or lower dropout probability, the effective participation approaches that of FedAvg, and the fallback deviation becomes negligible. Thus, fragment-based FedAvg retains the convergence behavior of FedAvg when fragment coverage is sufficiently high.

VI. EVALUATION

This section evaluates *UnlinkableDFL* in terms of learning performance, communication behavior, unlinkability, and resource usage. The experiments assess workflow stability under dynamic topologies, the effects of peer-based mixing on latency and unlinkability, and the computational cost introduced by continuous mixing. These results characterize the trade-offs between anonymity, model utility, and system overhead.

A. Experimental Setup

Each *UnlinkableDFL* node runs inside a Docker container and executes learning, routing, mixing, and monitoring tasks concurrently. Nodes communicate over Docker's internal virtual network using Docker's default bridge driver, which provides bidirectional TCP connectivity and allows the topology to adapt automatically when containers join or leave.

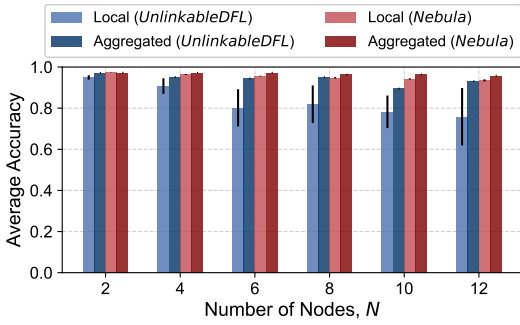


Fig. 2: Local and aggregated accuracy for UnlinkableDFL and Nebula across different numbers of nodes N .

The mixnet layer uses Sphinx-based onion routing with uniformly padded packets, random paths of up to $K = 2$ hops, and an outbox of size $O = 10$ for per-hop mixing. Transmission intervals follow a truncated normal distribution with mean $\mu = 0.005$ and standard deviation $\sigma = 0.001$, and cover messages are generated whenever the outbox becomes empty. Fragmentation splits model updates into 512-byte fragments prior to anonymous transmission. These settings represent the default configuration, while the evaluation also investigates the effect of varying O , μ , and K on latency, throughput, and unlinkability.

The default experiments use $N = 6$ nodes in a fully connected topology. Each node trains a small convolutional model (three Conv-BatchNorm-ReLU blocks, adaptive pooling, and a fully connected classifier) on MNIST, partitioned non-IID using a Dirichlet distribution with $\alpha = 10$. Training uses Adam with learning rate 10^{-3} , batch size 64, weight decay 10^{-4} , and standard augmentation. Experiments run for ten rounds, and all metrics are collected through the system’s built-in monitoring and logging components. Beyond the default node number $N = 6$, the evaluation also examines how different node numbers N affect system behavior and model accuracy, and compares convergence characteristics against the *Nebula* [5] baseline.

All experiments are executed on an Ubuntu 22.04 server with an AMD EPYC 7502P 32-core processor, 125 GB of RAM, and 197 GB of storage, without GPU acceleration.

B. Convergence and Learning Performance

The first experiment evaluates whether fragment-based aggregation and continuous mixing affect the learning behavior of DFL. Figure 2 reports the average local and aggregated accuracy for *UnlinkableDFL* across different numbers of nodes N , and compares the results to the *Nebula* baseline, which performs decentralized training using normal FedAvg without anonymous communication.

For each value of N , the darker bars represent aggregated accuracy and the lighter bars represent local accuracy, with error bars indicating the variance across nodes. The comparison shows that aggregated accuracy under *UnlinkableDFL* remains close to *Nebula*, and the variance across nodes remains small.

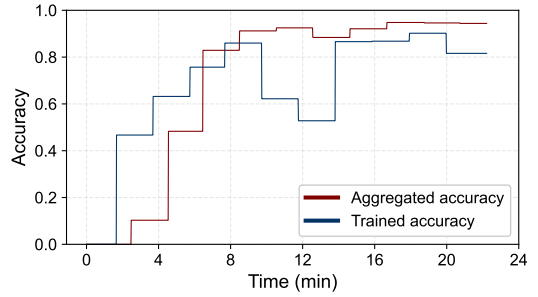


Fig. 3: Aggregated and local accuracy over time in *UnlinkableDFL*.

The separation between local and aggregated accuracy is consistent when anonymous routing or fragmentation is enabled.

Across different numbers of nodes, the aggregated accuracy of *UnlinkableDFL* stays above 0.85, even when nodes increase to $N = 12$. This indicates that fragment splitting does not significantly affect convergence. These observations align with the analysis in Section V-B, which is fragment-based FedAvg converges similarly to standard FedAvg as long as fragment coverage remains high and fallback deviation stays bounded.

Figure 3 shows the temporal convergence behavior of *UnlinkableDFL*. The aggregated model progresses in distinct steps and reaches its final accuracy earlier than the individual local models, indicating that fragment-based averaging reduces the variance present in local updates and stabilizes training over time.

C. Unlinkability Evaluation

This experiment evaluates how the mixnet parameters, the outbox size O and the maximum path length K , affect unlinkability. A controlled experiment is used: when varying O , K is fixed to its default value $K = 2$, and when varying K , the outbox size is fixed to $O = 10$. The analysis considers both relay entropy and end-to-end path entropy.

Figure 4 shows the relay entropy over the O and K . Increasing the outbox size leads to a steady rise in relay entropy, reflecting a larger candidate set during each mixing operation. Entropy increases from approximately 2–3 bits at

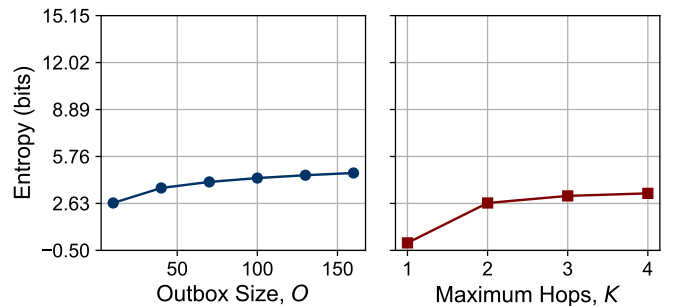


Fig. 4: Relay entropy over the outbox size O (left) and maximum hops K (right).

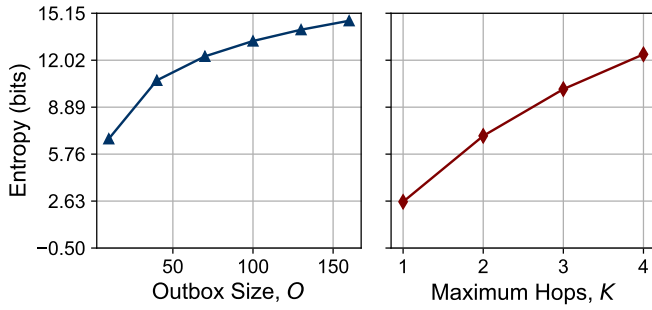


Fig. 5: End-to-end path entropy over the outbox size O (left) and maximum hops K (right).

$O = 10$ to above 4 bits at $O = 150$. This pattern matches the theoretical per-hop matching bound $\frac{K-1}{K} \cdot \frac{1}{O}$, where larger O reduces an adversary’s ability to correlate inputs and outputs at a single relay. A similar trend appears when varying K . Increasing the path length from $K = 1$ to $K = 2$ yields the largest improvement in relay entropy, as packets undergo an additional independent shuffle. Beyond two hops, the gain becomes smaller, consistent with diminishing marginal increases in per-hop uncertainty.

Figure 5 shows the total path entropy, which captures the number of indistinguishable source–destination paths consistent with the observed traffic. Path entropy grows significantly with O , rising from roughly 6 bits at $O = 10$ to above 14 bits at $O = 150$. This reflects the multiplicative growth of possible paths, approximated by $\log\left(\sum_{k=1}^K O^k\right)$. Larger outbox sizes expand the global anonymity set. Increasing K also increases total path entropy. The most substantial gain occurs between $K = 1$ and $K = 3$. The relationship reflects that longer paths introduce more mixing events but also incur additional delay.

D. Robustness to Topology Dynamics

This experiment evaluates how *UnlinkableDFL* behaves under dynamic topologies where nodes join or leave during training. The left part of Figure 6 shows the number of active neighbors (peers) observed by each node over time. Node 0 joins the system at minute 4, increasing the peer count of all other nodes. Node 1 leaves at minute 9, causing an immediate

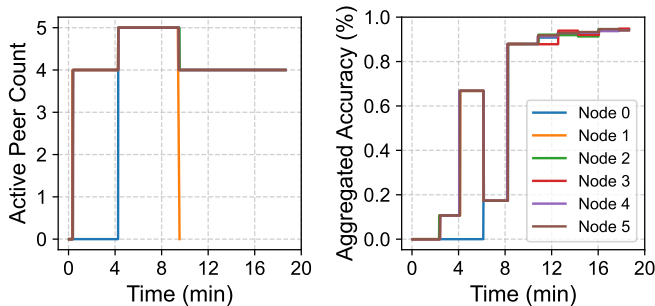


Fig. 6: Active peer count (left) and aggregated accuracy (right) over time as nodes join and leave the system.

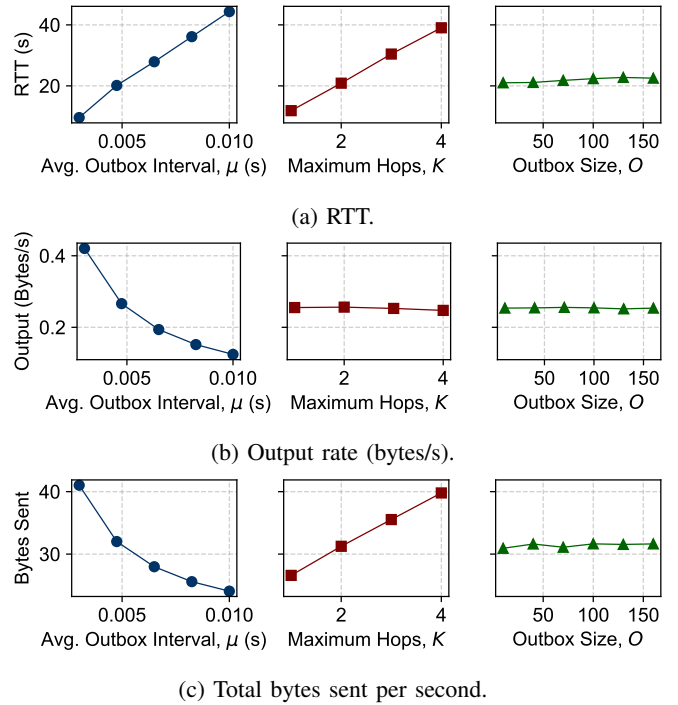


Fig. 7: Communication metrics under different μ , K , and O .

reduction in the active peer sets. All remaining nodes detect these changes within a short interval, indicating that the underlying communication layer updates local topology views promptly without external coordination.

The right part of Figure 6 illustrates the aggregated accuracy for each node under the same scenario. When a new node joins at minute 4, its underfitted model temporarily reduces the aggregated accuracy; after which, the system quickly recovers as the node completes its initial local updates. In contrast, the departure of node 1 at minute 9 produces no visible effect on the accuracy curves, and the remaining nodes continue to progress at the same rate. This behavior demonstrates that fragment-based aggregation effectively absorbs transient disturbances caused by late-joining nodes, and node departures do not disrupt model convergence.

E. Communication Overhead and Latency

This experiment analyzes the communication overhead introduced by the mixnet and fragment-based transmission. The evaluation considers three metrics under stationary traffic: round-trip time (RTT), steady-state output rate at each node, and total bytes sent per second, including cover traffic.

Figure 7a shows the RTT as a function of the average outbox interval μ , the maximum path length K , and the outbox size O . Increasing μ leads to a roughly linear increase in RTT, as packets wait longer in the outbox before transmission. Increasing K has a similar effect: each additional hop adds one more mixing and forwarding step, which accumulates in the end-to-end delay. In contrast, varying O has only a

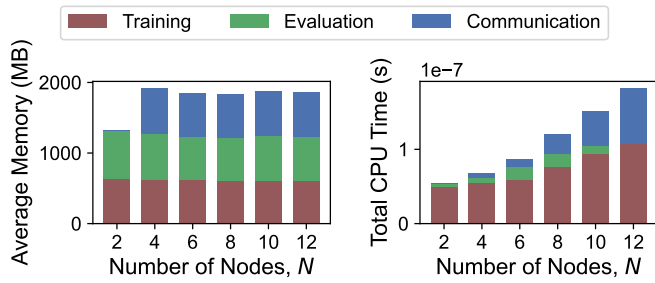


Fig. 8: Average memory consumption (left) and CPU time (right) as the number of nodes increases.

minor impact on RTT, since the outbox shuffle is lightweight compared to the fixed per-hop delay.

Figure 7b reports the steady-state output rate (throughput) in bytes per second. As μ increases, the throughput decreases, which is expected because nodes emit packets less frequently. However, changing the number of hops K does not alter the sending rate at each node. The outbox size O has minimal influence on the output rate, indicating that increasing the mixing set does not create a bandwidth bottleneck.

Figure 7c shows the total bytes sent per second. Smaller μ values produce higher traffic volume due to more frequent transmissions and, consequently, more cover packets. Increasing K raises the total bytes sent because each packet is carried across more links, while changes in O have little effect. Taken together, these measurements indicate that communication overhead is primarily controlled by the temporal parameter μ and the path length K , whereas increasing the outbox size O can improve unlinkability with comparatively little cost in latency or bandwidth.

F. Resource Consumption and Trade-off Analysis

Figure 8 shows the average memory consumption and CPU time per node as the number of participants increases. Memory usage grows moderately with N , and remains below 2 GB for all configurations. The memory is dominated by the training and evaluation components, while the communication layer contributes a smaller but stable portion. In terms of the CPU time, both training and communication costs grow with the number of nodes, and the communication component becomes more pronounced as more relays are active. This reflects the cumulative cost of onion encryption, decryption, mixing, and fragment handling, which scale with the number of concurrent paths in the overlay.

Figure 9 compares the round duration of *UnlinkableDFL* with *Nebula*. *UnlinkableDFL* incurs longer round times due to multi-hop forwarding, randomized delays, and cover traffic. As N grows, this communication cost becomes the dominant scalability constraint. Overall, the results indicate that unlinkability is achieved at the expense of higher communication latency, while memory and CPU overheads remain moderate and stable across different node counts.

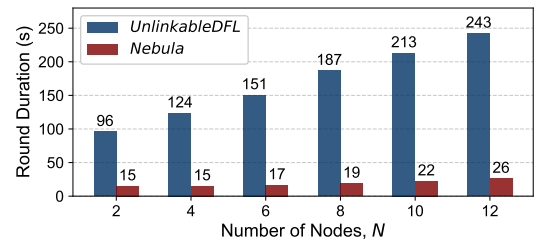


Fig. 9: Round duration for UnlinkableDFL and Nebula as the number of nodes increases.

VII. CONCLUSION AND FUTURE WORK

This paper presented *UnlinkableDFL*, a DFL framework that integrates a peer-based mixnet with fragment-based aggregation to provide unlinkability without relying on a central coordinator. The system maintains comparable convergence to standard DFL, tolerates topology changes, and achieves measurable relay and end-to-end unlinkability. The evaluation shows that unlinkability primarily increases communication latency, while memory and CPU overheads remain moderate.

Future work includes reducing the communication latency through adaptive routing and rate control, incorporating lightweight cryptographic primitives to lower per-hop processing cost, and exploring anonymity-preserving federated optimization methods that further reduce dependence on synchronous communication. Extending the system to heterogeneous device settings and large-scale deployments is another direction for improving practical applicability.

REFERENCES

- [1] S. Abdulrahman, H. Tout, H. Ould-Slimane, A. Mourad, C. Talhi, and M. Guizani, "A survey on federated learning: The journey from centralized to distributed on-site learning and beyond," *IEEE Internet of Things Journal*, vol. 8, no. 7, pp. 5476–5497, 2021.
- [2] B. McMahan, E. Moore, D. Ramage, S. Hampson, and B. A. y Arcas, "Communication-efficient learning of deep networks from decentralized data," in *Artificial intelligence and statistics*, pp. 1273–1282, 2017.
- [3] J. Kang, Z. Xiong, D. Niyato, Y. Zou, Y. Zhang, and M. Guizani, "Reliable federated learning for mobile networks," *IEEE Wireless Communications*, vol. 27, no. 2, pp. 72–80, 2020.
- [4] E. T. Martínez Beltrán, M. Q. Pérez, P. M. S. Sánchez, S. L. Bernal, G. Bovet, M. G. Pérez, G. M. Pérez, and A. H. Celdrán, "Decentralized federated learning: Fundamentals, state of the art, frameworks, trends, and challenges," *IEEE Communications Surveys & Tutorials*, vol. 25, no. 4, pp. 2983–3013, 2023.
- [5] E. T. Martínez Beltrán, Ángel Luis Perales Gómez, C. Feng, P. M. Sánchez Sánchez, S. López Bernal, G. Bovet, M. Gil Pérez, G. Martínez Pérez, and A. Huertas Celdrán, "Fedstellat: A platform for decentralized federated learning," *Expert Systems with Applications*, vol. 242, p. 122861, 2024.
- [6] C. Feng, N. F. Kohler, Z. Wang, W. Niu, A. H. Celdran, G. Bovet, and B. Stiller, "Colnet: Collaborative optimization in decentralized federated multi-task learning systems," 2025.
- [7] J. Zhang, M. Li, S. Zeng, B. Xie, and D. Zhao, "A survey on security and privacy threats to federated learning," in *2021 International Conference on Networking and Network Applications (NaNA)*, pp. 319–326, 2021.
- [8] C. Feng, Y. Gao, A. H. Celdran, G. Bovet, and B. Stiller, "From models to network topologies: A topology inference attack in decentralized federated learning," in *28th European Conference on Artificial Intelligence (ECAI)*, pp. 1–8, 2025.
- [9] A. M. Piotrowska, J. Hayes, T. Elahi, S. Meiser, and G. Danezis, "The loopix anonymity system," in *26th usenix security symposium (usenix security 17)*, pp. 1199–1216, 2017.

- [10] N. K. Jadav, R. Gupta, P. Bhattacharya, and S. Tanwar, "Fedonion: FI and onion routing-driven secure data exchange framework for 5g-iiot applications," in *GLOBECOM 2023-2023 IEEE Global Communications Conference*, pp. 7315–7320, IEEE, 2023.
- [11] Y. Chen, Y. Su, M. Zhang, H. Chai, Y. Wei, and S. Yu, "Fedtor: An anonymous framework of federated learning in internet of things," *IEEE Internet of Things Journal*, vol. 9, no. 19, pp. 18620–18631, 2022.
- [12] S. Steinbrecher and S. Köpsell, "Modelling unlinkability," in *International workshop on privacy enhancing technologies*, pp. 32–47, 2003.
- [13] T. Orekondy, S. J. Oh, Y. Zhang, B. Schiele, and M. Fritz, "Gradient-leaks: Understanding and controlling deanonymization in federated learning," *arXiv preprint arXiv:1805.05838*, 2018.
- [14] M. Lam, G.-Y. Wei, D. Brooks, V. J. Reddi, and M. Mitzenmacher, "Gradient disaggregation: Breaking privacy in federated learning by reconstructing the user participant matrix," in *International Conference on Machine Learning*, pp. 5959–5968, PMLR, 2021.
- [15] J. Chen, Z. Si, J. Song, M. Mohanty, W. Wang, and H. Xiong, "Ufl: Unlinkable federated learning through shuffle and shamir's secret sharing," in *International Conference on Advanced Data Mining and Applications*, pp. 239–253, Springer, 2024.
- [16] X. Chen, Y. Gao, and H. Deng, "Aifl: ensuring unlinkable anonymity and robust incentive in cross-device federated learning," *IEEE Internet of Things Journal*, vol. 11, no. 22, pp. 36688–36702, 2024.
- [17] G. Almashaqbeh and Z. Ghodsi, "Anofel: Supporting anonymity for privacy-preserving federated learning," *Proceedings on Privacy Enhancing Technologies*, vol. 2, pp. 88–106, 2025.
- [18] D. Chaum, D. Das, F. Javani, A. Kate, A. Krasnova, J. De Ruiter, and A. T. Sherman, "cmix: Mixing with minimal real-time asymmetric cryptographic operations," in *International conference on applied cryptography and network security*, pp. 557–578, Springer, 2017.
- [19] D. L. Chaum, "Untraceable electronic mail, return addresses, and digital pseudonyms," *Communications of the ACM*, vol. 24, pp. 84–90, 1981.
- [20] K. Sampigethaya and R. Poovendran, "A survey on mix networks and their secure applications," *Proceedings of the IEEE*, vol. 94, no. 12, pp. 2142–2181, 2007.
- [21] M. Jakobsson and A. Juels, "An optimally robust hybrid mix network," in *Proceedings of the twentieth annual ACM symposium on Principles of distributed computing*, pp. 284–292, 2001.
- [22] B. Möller, "Provably secure public-key encryption for length-preserving chaumian mixes," in *Cryptographers' Track at the RSA Conference*, pp. 244–262, Springer, 2003.
- [23] A. Blanco-Justicia, J. Domingo-Ferrer, S. Martínez, D. Sánchez, A. Flanagan, and K. E. Tan, "Achieving security and privacy in federated learning systems: Survey, research challenges and future directions," *Engineering Applications of Artificial Intelligence*, vol. 106, p. 104468, 2021.
- [24] Y. Chen, Y. Su, M. Zhang, H. Chai, Y. Wei, and S. Yu, "Fedtor: An anonymous framework of federated learning in internet of things," *IEEE Internet of Things Journal*, vol. 9, no. 19, pp. 18620–18631, 2022.
- [25] X. Wang, J. Li, H. Lin, C. Dai, S. Garg, and G. Kaddoum, "Aefl: Anonymous and efficient federated learning in vehicle road cooperation systems with augmented intelligence of things," *IEEE Internet of Things Journal*, 2024.
- [26] T. Li, A. K. Sahu, M. Zaheer, M. Sanjabi, A. Talwalkar, and V. Smith, "Federated optimization in heterogeneous networks," *Proceedings of Machine learning and systems*, vol. 2, pp. 429–450, 2020.
- [27] S. P. Karimireddy, S. Kale, M. Mohri, S. Reddi, S. Stich, and A. T. Suresh, "Scaffold: Stochastic controlled averaging for federated learning," in *International conference on machine learning*, pp. 5132–5143, PMLR, 2020.

All links above were last accessed on February 26, 2026.